ENVIRONMENTAL RESEARCH
LETTERS

LETTER • OPEN ACCESS

A compound event-oriented framework to tropical fire risk assessment in a changing climate

ENVIRONMENTAL RESEARCH
LETTERS

OPEN ACCESS

RECEIVED
3 December 2021

REVISED
25 April 2022

ACCEPTED FOR PUBLICATION
25 May 2022

PUBLISHED
10 June 2022

LETTER

A compound event-oriented framework to tropical fire risk assessment in a changing climate

Andreia F S Ribeiro[1,*], Paulo M Brando[2,3,4], Lucas Santos[2,3], Ludmila Rattis[3,4], Martin Hirschi[1], Mathias Hauser[1], Sonia I Seneviratne[1] and Jakob Zscheischler[5,6,7]

[1] Institute for Atmospheric and Climate Science, Department of Environmental Systems Science, ETH Zurich, Universitätstrasse 16, 8092 Zurich, Switzerland
[2] Department of Earth System Science, University of California, Irvine, CA, United States of America
[3] Instituto de Pesquisa Ambiental da Amazônia (IPAM), Brasília-DF 71503-505, Brazil
[4] Woodwell Climate Research Center, Falmouth, MA 02540-1644, United States of America
[5] Department of Computational Hydrosystems, Helmholtz Centre for Environmental Research—UFZ, Leipzig, Germany
[6] Climate and Environmental Physics, University of Bern, Bern, Switzerland
[7] Oeschger Centre for Climate Change Research, University of Bern, Bern, Switzerland
[*] Author to whom any correspondence should be addressed.

E-mail: andreia.ribeiro@env.ethz.ch

Keywords: fire risks, compound events, global warming, Xingu, Pantanal

Supplementary material for this article is available online

Abstract

Tropical fire activity closely follows the co-occurrence of multiple climate stressors. Yet, it remains challenging to quantify how changes in climate alter the likelihood of fire risks associated with compound events. Recent abrupt changes in fire regimes in iconic landscapes in Brazil (namely the Pantanal and Xingu) provide a key opportunity to evaluate how extremely dry and hot conditions, both together and individually, have influenced the probability of large fires. Here we quantify the relationships between climate and fire across these regions and provide evidence on the extent to which fire risk and the associated impacts could be constrained if anthropogenic global warming is limited. We investigate the burned area, differentiating between fire types according to land use (forest fires, savanna fires, farming fires and grassland and wetland fires), and derive present and future fire risks linked to multiple climate variables. We show that concurrent air dryness (high vapour-pressure deficit (VPD)) and low precipitation have driven fire occurrence in both Xingu and the Pantanal, with VPD playing a dominant role. Historical climatic change has already increased compound event-related (CE-related) fire risks of all fire types (5%–10%), and these risks are likely to increase in the future due to global warming. The likelihood of CE-related increase in fire risk may be reduced by up to 14.4% if global warming is constrained to +1.5 °C instead of +3 °C. Nevertheless, substantially increased CE-related fire risks are still expected even if restricting global mean warming to 1.5 °C, particularly in the Pantanal. We thus conclude that climate action should be coordinated with environmental protection to reduce ignition sources and promote effective conservation measures to preserve these biomes.

1. Introduction

A complex interplay between climate variability and human activities controls most of the contemporary fire regime of tropical ecosystems [1–4]. In recent decades, extremely dry and warm years have triggered wildfires that were larger, more intense and more severe than during years with normal climate conditions [5, 6]. Combined with high deforestation rates and increasing agricultural expansion, the impacts of forest degradation have been exacerbated by the combination of concurrent warm and dry conditions and human activities that increase ignition sources and fuel loads [7]. This creates a positive feedback loop where rapid change in climate and land use leads to fundamental shifts in fire regimes, degradation of tropical forests and savannas, and dryer and more flammable landscapes [8]. The combination of these factors has made widespread wildfires during extremely dry and warm years increasingly common

[6, 9–11]. Of particular concern is that climate change is expected to reinforce this downward spiral of socio-environmental impacts across the tropics, threatening the terrestrial carbon cycle, the hydrological cycle, biodiversity, the livelihood of indigenous peoples [12] and other traditional communities [13].

Iconic landscapes in Brazil, namely the Xingu Basin and the Pantanal, are expected to become more flammable in a future drier and warmer climate in combination with human-modified landscapes, and thus particularly vulnerable to a 'gathering firestorm' [10]. Both regions house stakeholders lacking resources to properly manage fire outbreaks associated with novel fire regimes, and a generalized lack of governmental action to mitigate this crisis has jeopardized the livelihood of the populations living in those regions.

Located in the ecotone between the Amazonia and Cerrado biomes, the Xingu region is hypothesized to become vulnerable to transitions from forest into drier environment with more sparse vegetation, and an intensification of the region's fire regimes due to climate change may already be underway [14]. In the same manner, the Pantanal has been increasingly degraded by fires [15, 16] and abrupt changes in its fire regimes could drive large-scale vegetation degradation, with catastrophic consequences for biodiversity [15, 17–19]. In combination with the lack of sustainable environmental and conservation practices, climate change might exacerbate the decreasing resilience during extremely dry and warm years, resulting in many negative social and environmental consequences across these biocultural heritage sites.

The frequency and intensity of co-occurring droughts and atmospheric aridity will likely continue to increase with global warming [20, 21], however, it is still unclear how they will affect the probability of fire activity across different land uses in the tropics. Compound dry and hot conditions have substantial negative impacts on tropical ecosystems by increasing the likelihood of widespread fires, but few studies have quantified the relationship between compound events and tropical fire activity (for tropical regions see [22–24] and for other regions see e.g. [25–27]). In principle, multivariate events characterized by co-occurring droughts, heat waves, and increased atmospheric water demand could drive nonlinear (e.g. exponential) increases in fire activity, mostly due to land-feedback mechanisms [28]. One of the major challenges in this respect is the identification of the meteorological drivers of fire activity and the thresholds beyond which fires become extreme, to enhance our understanding of what permits fires to spread out of control. Another challenge involves quantifying the dependencies of such drivers, which are likely to change under strong greenhouse gas forcing [29]. Instead, most of the impact-centric studies disregard changes in the distribution of the climate drivers in the different future pathways. To address this gap, we adopt a compound event-oriented framework to fire risk assessment in this work [30], accounting for the interactions between hydrometeorological drivers of fire occurrence.

The main goal of the present study is to characterize compounding drivers of fire activity and to quantify the compound event-related (CE-related) fire risk in present-day and future climate in Xingu and the Pantanal, providing evidence on the need to constrain global mean warming. To foster mitigation of climate- and human-induced fire risks, it is important to improve our understanding of what triggers and regulates high-intensity tropical fires across these key regions, and how changes in climate may alter their likelihood in the future [1, 31–33].

2. Data and methods

2.1. Study regions

We focus on two distinct tropical regions in Brazil, namely the Upper Xingu basin in south eastern Amazonia and the Pantanal (figures 1(e) and S1 (available online at stacks.iop.org/ERL/17/065015/mmedia)). The Xingu region includes areas across the Amazonia-Cerrado region, and the Xingu Indigenous Park, one of the largest indigenous conservation areas in Brazil. This reserve is home to 6000 indigenous people from 16 ethnicities belonging to 5 linguistic families and greatly contributes to the conservation of the standing rainforest and to the stabilization of the local climate [34]. The Xingu region is particularly threatened by agricultural expansion around the edges (figures 1(e) and S1), and this growing agricultural frontier is expected to become drier and warmer in the future [34–36]. Most widespread high-intensity wildfires come from intentional agricultural or deforestation fires, which may ignite wildfires. In dry and hot years, some of these wildfires may run out of control and burn large forested areas. However, despite an observed decline in deforestation during 2007 and 2010, the Xingu region experienced major intensive and widespread fire activity triggered by dryness acting together with elevated temperatures [3, 10, 12]. This suggests the paramount role of climate and the vulnerability of this region to dry and hot conditions, even under the suppression of ignition sources associated with deforestation [10].

The Pantanal is the world's largest continuous tropical wetland. It consists of a very complex and diverse ecosystem, sharing borders with the Amazonia, Cerrado and Chaco biomes and housing seven native indigenous populations (figures 1(e) and S1). The Pantanal's burned area between 1985 and 2020 exceeded all the other Brazilian biomes [37], and during the anomalous dry and warm year of 2020, nearly 30% of the Biome was burned, affecting at least 65 million vertebrates [38], directly killing 17 million of them [19]. In 2020, the fire season across the

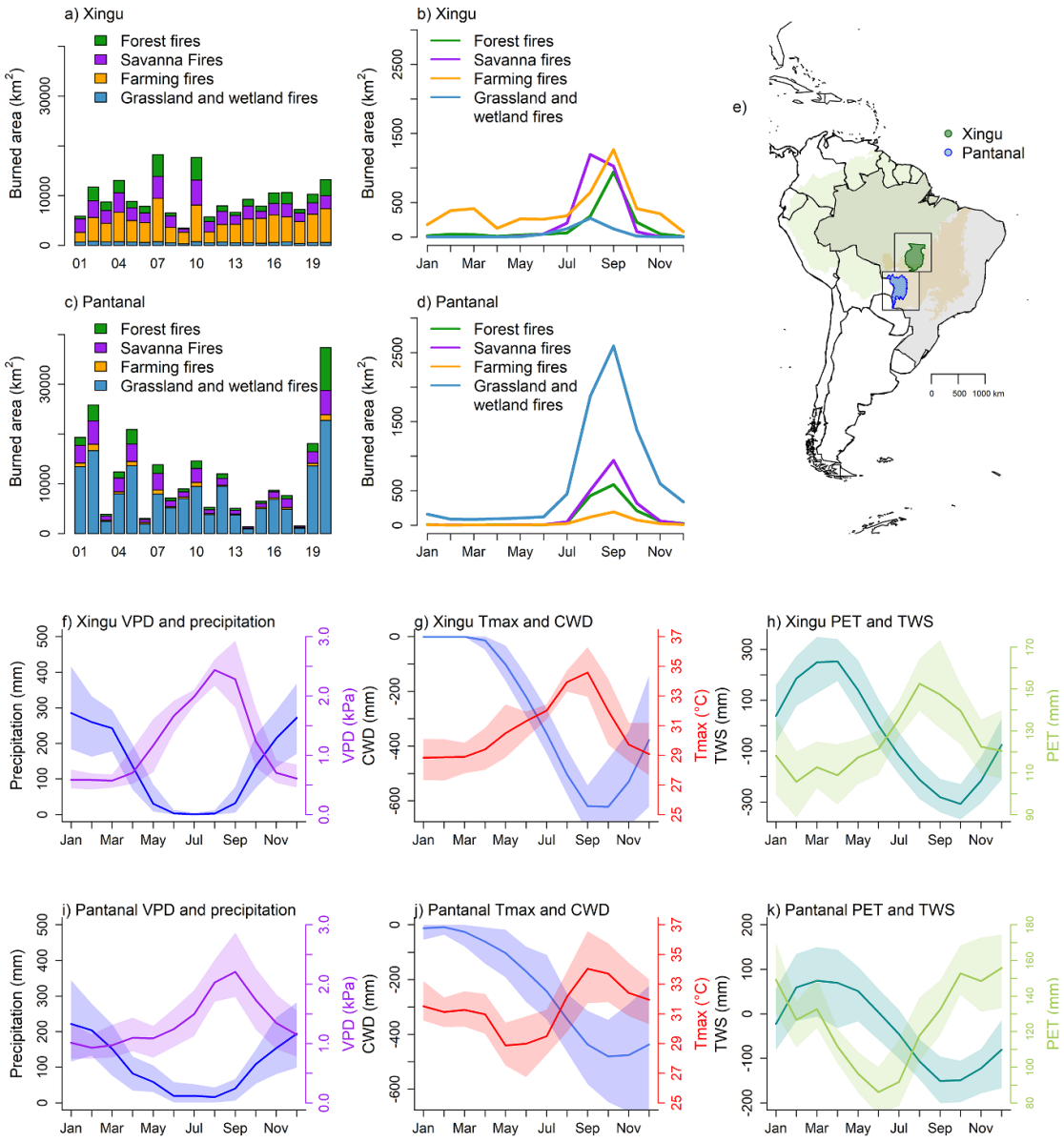

Figure 1. Burned area by land use and hydrometeorological drivers during 2001–2020. Annual amounts (a), (c) and mean annual cycle (b), (d) of burned area by land use comprising forest fires (green), savanna fires (purple), farming fires (orange) and grassland and wetland fires (blue), during 2001–2020 in Xingu (a), (b) and the Pantanal (c), (d). (e) Location of the Upper Xingu basin (dark green) and the Pantanal (blue) in relation to Brazil (grey) and the biomes of Amazonia (light green) and Cerrado (light brown), surrounded by the respective CMIP6 domain box (black squares). Mean annual cycle of precipitation (f), vapour-pressure-deficit (VPD) (f), cumulative water deficit (CWD) (g), maximum temperature (Tmax) (g), terrestrial water storage (TWS) (h) and potential evapotranspiration (PET) (h) across Xingu (f)–(h) and the Pantanal (i)–(k). Shading in (f)–(k) illustrates the range between the 5th and 95th percentile of each month during 2001–2020 (2001–2019 in the case of TWS).

Pantanal has reached striking records of fire activity, with an increase of about six times the annual cumulative number of fires in relation to the 2012–2019 average [15–17]. The dry 2019 and 2020 in the Pantanal were induced by unusually warm waters in the tropical North Atlantic, decreasing summer precipitation by ∼60% and depleting water levels across the basin [5].

2.2. Burned area by land use and climate datasets

To investigate burned area by land use, we combine the MODIS-derived MCD64A1 monthly burned area product during 2001–2020 [39] and the annual MapBiomas Collection 6 land-cover maps during 2001–2020 [40] (https://mapbiomas.org) in Google Earth Engine. MapBiomas is a land-use mapping initiative carried out by multiple institutions based on remote sensing and local knowledge, available for Brazil and other tropical countries, widely used across Brazil for research and decision-making processes. We apply monthly masks of detected burned areas to the respective annual land cover maps (figure S1) and count the number of burned pixels per land cover subclass inside the borders of Xingu and the Pantanal (figures S2 and S3). For convenience and to allow comparison between the two regions, we merge

the available subclasses of burned pixels by land use to characterize the fire activity in terms of 'forest fires', 'savanna fires', 'farming fires' and 'grassland and wetland fires' (see table S1). More details about the MODIS and MapBiomas datasets can be found in the supplementary material S1.

To characterize the burned area response to climate we consider a suite of hydrometeorological variables including monthly means of daily maximum (Tmax), vapour-pressure deficit (VPD), potential evapotranspiration (PET), monthly accumulated precipitation, cumulative water deficit (CWD) from ERA5-Land [41] as well as GRACE terrestrial water storage (TWS) reconstructions from [42]. To further analyse projections of CE-related fire risks, we use Coupled Model Intercomparison Project Phase 6 (CMIP6 [43]) centennial simulations from 14 Earth system models (ESMs). We only analyse simulations from the shared socioeconomic pathways (SSPs) projection [44] SSP5-8.5 for global warming levels (GWLs) of +1.5 °C, +2.0 °C, and +3.0 °C, expressed relative to the period 1850–1900 [45, 46]. The 14 models are selected based on availability of the required archived variables for analysis. The SSP5-8.5 is chosen to ensure that all models reach the considered GWLs. For each model individually, the GWL time-period corresponds to the first 20 year period where the global mean temperature is on average above the temperature level. In this way, the time period of each GWL is different in every model, which greatly reduces the differences between emission scenarios for many variables [47].

Spatial averages of each climate variable are considered as explanatory variables in further modelling of the burned area by land use over the regions of Xingu and the Pantanal. More details about the different climate datasets can be found in the supplementary material S1.

2.3. Statistical analysis

2.3.1. Burned area response to climate

We model monthly burned area by land use as a function of hydrometeorological variables using a Poisson regression model with a logarithmic link function for local likelihood fitting [23, 48, 49]. Previous work by [23] found Poisson regression to be suitable to describe the non-linear role of temperature and precipitation on fire counts in Amazonia. Here we extend this approach to burned area by land use as a function of single and pairs of climate variables. More details about local likelihood Poisson regression are given in the supplementary material S2.

The relationship between burned area by land use and single climate variables is first evaluated individually for VPD, Tmax, PET, precipitation, CWD (during 2001–2020) and TWS (2001–2019). Second, combinations of water and temperature related variables are considered, pairing drought and heat-related metrics: (precipitation, VPD), (precipitation, Tmax), (precipitation, PET), (CWD, VPD), (CWD, Tmax), (CWD, PET), (TWS, VPD), (TWS, Tmax), (TWS, PET). The selection of these variables to characterize compound drivers of fire is motivated by the assumption that climate-driven fire risk is primarily modulated by the surface soil-, deep soil- and air-dryness. These deplete surface and groundwater levels and increase evaporative demand, leading to plant water stress and thus increasing fuel loads as plants shed leaves and twigs as they die [50].

To compare different statistical models, we consider the Akaike information criteria (AIC) and R-squared, which is determined as the square of the correlation between fitted values and observations. Based on the two metrics, we first compare the non-linear response of burned area between single climate variables. According to the best predictive skill, the univariate model characterizing the response of burned area to VPD individually is selected as the 'benchmark' model (as will be detailed in the section 3 and figure 2). Based on this benchmark, we test whether using the multivariate models characterizing compound drivers of fire leads to higher R-squared and lower AIC values.

As further detailed in the section 3, we restrict the subsequent assessments to bivariate distributions of VPD and precipitation, because precipitation is a readily available variable in CMIP6 models and result in similar performance as the best statistical models. Fire risk in different time periods was estimated based on 20 year periods in the present (2001–2020), past (1981–2000) and future (different warming levels expressed relative to 1850–1900). In particular, we estimate the probability of crossing burned area extremes as explained below.

2.3.2. CE-related fire risk

CE-related fire risk is defined as the likelihood of burned area extremes predicted by multiple fire drivers, here VPD and precipitation. The probability of exceeding a critical threshold of burned area is obtained empirically by counting the relative number of occurrences of VPD and precipitation for which burned area exceeds its 90th percentile based on the Poisson regression model fitted for the reference period (present, see section 2.3.1). Hence, for the present time period (2001–2020), fire risk is 10% by construction in a perfect model. To obtain a robust number in particular of the tail occurrences of VPD and precipitation, 10 000 samples are drawn from parametric fits of the bivariate distribution of VPD and precipitation [51] (see supplementary material S4). Uncertainties associated with the fitting of the parametric bivariate distribution are estimated by repeated sampling (1000 times) with sample sizes equal to the number of observations (12 months times 20 years equals $N = 240$). From these samples, we show the range between the 2.5% and 97.5% percentile to provide a 95% confidence interval.

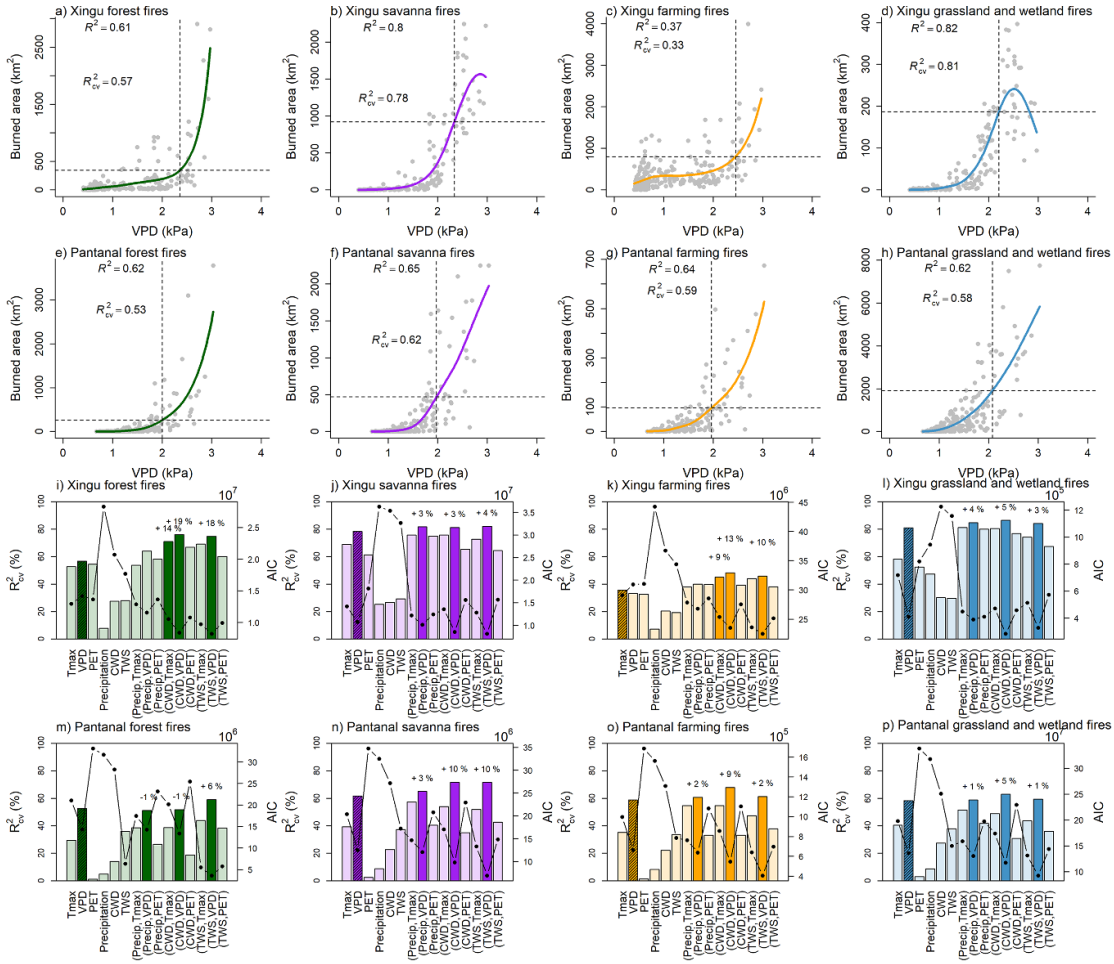

Figure 2. Burned area responses to single and couples of hydrometeorological variables in Xingu and the Pantanal during 2001–2020. The response of forest fires (a), (e), savanna fires (b), (f), farming fires (c), (g) and grassland and wetland fires (d), (h) to VPD across Xingu (first row, (a)–(d)) and the Pantanal (second row, (e)–(h)). The horizontal black dashed line denotes the 90th percentile of burned area, and the vertical black dashed line indicates the associated threshold of VPD. Goodness of fit metrics of the local likelihood Poisson regression models with individual and combinations of hydrometeorological variables, Xingu (third row, (i)–(l)) and the Pantanal (bottom row, (m)–(p)) forest fires (i), (m), savanna fires (j), (n), farming fires (k), (o) and grassland and wetland fires (l), (p). Colour bars indicate the squared correlation between observations and fitted values with cross-validation scheme (R^2_{cv}) and the black line indicates the Akaike information criteria (AIC). The dark-coloured textured bar denotes the best model among those with a single predictor (VPD in all cases, except for farming fires)—i.e. the benchmark model—and the dark-coloured bars denote the best three models among those with pairs of predictors. The increase in explained variance of the multivariate models in comparison to the benchmark model is indicated on top of the right-side dark-coloured bars.

We further consider potential climate model biases in the simulation of bivariate distributions of VPD and precipitation as an additional source of uncertainty. Specifically, for each region we generate samples from three different parametric bivariate distributions based on three different ways to adjust biases in the CMIP6 data (supplementary material S5). First we consider a simple univariate bias-correction (UBC) which corrects VPD and precipitation individually based on quantile delta mapping [52] and we use the dependence structure (copula) of the observations to link the two (UBC (C_{obs})). Secondly, we use the same UBC approach to bias-adjust VPD and precipitation individually but using the dependence structure of the climate models under future conditions (UBC (C_{raw})). Finally, we use a multivariate bias-correction approach [53] that adjusts both the VPD and precipitation individually, in addition to adjusting the dependence structure of the climate model to fit the observations. We typically report the climate model average value of the CE-related fire risk as the best estimate. 95% confidence intervals are obtained by repeated sampling (see above) and include the model uncertainty (estimated from 1000 times 14 values).

It is worth noting that past and future fire risks are extrapolated from the present-day response surfaces, which are assumed to remain unchanged. In this way only changes in the climate drivers are considered. In other words, an occurrence is considered 'riskier' in terms of fire-critical impacts, when a larger number of concurrent air dryness and precipitation deficit realizations (from the respective bivariate distribution) is obtained, assuming no alterations in the response of

burned area to climate. More details about the proposed compound event-oriented framework can be found in the supplementary material S1–S5.

3. Results

3.1. General patterns of burned area in Xingu and the Pantanal

All types of fires (forest fires, savanna fires, farming fires and grassland and wetland fires) occurred every year (figures 1(a), (c) and S2, S3). The burned area peaked during the drought years 2007 and 2010 in Xingu while in the Pantanal the peak occurred in 2020, followed by 2005 and 2002 (figures 1(a) and (c)). In Xingu, ∼49% of the area burned during 2001–2020 is attributed to farming fires, followed by ∼27% from savanna fires, ∼18% from forest fires and ∼6% of grassland and wetland fires (figures 1(a) and (b), table S1). In contrast, more than 66% of the burned area in the Pantanal is caused by fires across grasslands and wetlands, followed by savanna, forest and farming fires (figures 1(c) and (d), table S1).

The annual cycles of burned area (figures 1(b) and (d)) show a marked seasonality across all fire types and in both regions, with most fires occurring between July and October, with the exception of farming fires, which tend to increase earlier in the year (figure 1(b)). While all types of fire in the Pantanal peak in September, in Xingu savanna, grassland and wetland fires peak in August, whereas forest and farming fires peak in September. Overall, the fire season months (July–October) in Xingu/Pantanal account for 87%/91% (forest fires), 97%/94% (savanna fires), 56%/86% (farming fires) and 91%/80% (grassland and wetland fires) of the total burned area during 2001–2020 (figure S4).

In both regions, the annual cycle of burned area (figures 1(b) and (d)) is closely related to the seasonality of climate (figures 1(f)–(k)). The seasonal cycle of pairs of heat and drought related metrics—(VPD, precipitation—figures 1(f) and (i)), (Tmax, CWD—figures 1(g) and (j)), (PET, TWS—figures 1(h) and (k))—indicates that the peaks of warm conditions coincide with dry conditions during peaks of burned area. This synchronicity suggests the importance of climate seasonality to the intra-annual variability of burned area. During the dry season when climate conditions are warm and dry, fire occurrence strongly increases.

3.2. Burned area is nonlinearly modulated by climate

The relationship between historical fire occurrence and individual hydrometeorological variables is mostly nonlinear (figures 2 and S5–S9). For example, burned area increases exponentially as a function of increasing VPD and Tmax (figures 2 and S5). This suggests climate thresholds beyond which the fire activity becomes extreme. In general, large fires (i.e. 90th percentile of the observed burned area; horizontal dashed lines) in the Pantanal occur with less severe droughts and heat conditions compared to the Xingu region, as shown by the vertical dashed lines in figures 2 and S5–S9. For example, VPD values triggering major increases in fire activity (∼2-2.5 kPa) are slightly lower in the Pantanal than in Xingu. Similarly, Tmax thresholds (figure S5—values between 33.4 °C and 34.2 °C) associated with widespread fires are slightly lower for the Pantanal, except for grassland and wetland fires. For PET, threshold values triggering large fires (between 132.7 mm and 177.8 mm) are also slightly lower in the Pantanal (except for grassland and wetland fires), but univariate relationships with PET do not explain fire activity well in this region (figure S6). Similarly, low TWS values (figure S9) are associated with high values of burned area and are not so extreme in the Pantanal (between −166.5 mm and −147.7 mm) compared to Xingu (between −315.5 mm and −208.6 mm).

An exception to the predominant exponential response of burned area to climate are fires across savannas, grasslands and wetlands in Xingu (except precipitation, figures 2(b), (d) and S5(b), (d)–S9(b), (d)), where extreme values of the explanatory variable lead to a reduction in the burned area. The fire response to CWD in the Pantanal (figures S8(e)–(h)), follows a similar nonlinear behaviour, where below −600 mm the CWD it is not a limiting factor anymore, and the interplay between multiple climate stressors can be relevant.

3.3. Burned area responses to compound drivers

VPD explains most variability in fire occurrence among the statistical models with single predictors, except for farming fires in Xingu (figures 2(i)–(p) bar with shading lines). Among all fitted models (univariate and multivariate), those accounting for the compounding effects of drought and heat, and including VPD, are the best models (figures 2(g)–(l), except for farming fires in Xingu), with gains of up to 19% in explained variance (figure 2(i)). Those models minimize the likelihood when penalizing the number of predictors, as indicated by the AIC values, which suggest that the increase in variance is not just a result from the increase in the number of predictors. The only exception is the case of forest fires in the Pantanal (figure 2(m)), where the bivariate statistical models based on (VPD, precipitation) and (VPD, CWD) display a decrease in 1% in explained variance, in comparison to the benchmark model based on VPD alone. Nevertheless, the AIC does not increase in those cases, and the bivariate statistical model based on (VPD, TWS) increases the variance, emphasizing the relevance of accounting for compound drivers of fire.

For the variables paired with VPD, the performance in terms of explained variance is generally similar between precipitation, CWD and TWS (figure 2). Because precipitation is a direct output in climate

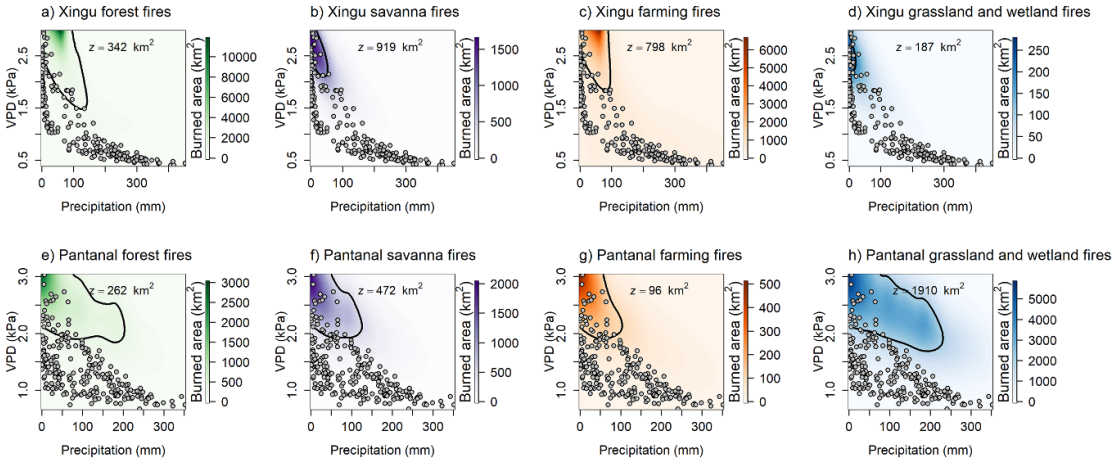

Figure 3. Surfaces of burned area response to concurrent monthly variations of VPD and precipitation during 2001–2020. Local likelihood Poisson regression of forest fires (a), (e), savanna fires (b), (f), farming fires (c), (g) and grassland and wetland fires (d), (h) across Xingu (top row, (a)–(d)) and the Pantanal (bottom row, (e)–(h)) as function of VPD and precipitation. The black contour line indicates the critical threshold of impact, defined as the 90th percentile of the observed burned area by land use, and the observed values of VPD and precipitation are superimposed onto each response surface (grey points).

models, we focus on the response surfaces as a function of VPD and precipitation for the remainder of this study. Figure 3 shows the modelled response surfaces of burned area by land use with respect to VPD and precipitation, for Xingu and the Pantanal. In all regions and fire types, burned area strongly increases with increasing VPD and decreasing precipitation. In general, the relationship between VPD and precipitation is exponential and negatively correlated, with higher values of VPD associated with lower values of precipitation. The bivariate regression models based on VPD and precipitation match observations relatively well in most cases (figure S10).

Similar to the univariate case, we illustrate the 90th percentile exceedance for burned area in the bivariate VPD-precipitation space with contour lines (figure 3). Regions of extremely high burned area coincide with very high VPD and very low precipitation. Consistent with the univariate analysis, VPD and precipitation need to be more extreme in Xingu than in the Pantanal to result in burned area extremes.

3.4. Present and future projection of CE-related fire risks

Present-day climate change has already led to more fire prone conditions in our study regions (figure 4). Fire risk, based on our statistical model, has increased from 1981–2000 to 2001–2020 for both regions and all fire types (table 1). This is also illustrated in figure 4 for forest fires/grassland and wetland fires (8.5%/9.8%) in Xingu/Pantanal (i.e. the fire types with the most increase in fire risk with present-day climate change—table 1). Future climate change is also projected to further increase fire risk for all regions and fire types (figure 5). The only exception are grassland and wetland fires in Xingu, which show a slight decrease from +1.5 °C to +2 °C, and from +2 °C to +3 °C (figure 5(c)), suggesting that area burned by this type of fires may decrease with global mean warming above 2 °C. This may be related with the shape of the response surface in figure 3(c), which suggests that reductions in the burned area are expected above ∼3 kPa VPD.

In general, CE-related fire risks in absolute magnitude and in terms of changes relative to 2001–2020 are consistently higher in the Pantanal than in Xingu (figure 5 and table 1). Most future changes in CE-related fire risk relative to 2001–2020 are expected to be greater than already observed past to present-day increases (from 1981–2000 to 2001–2020, see figures 4, 5 and table 1) in both regions. Besides grassland and wetland fires, the other exception are savanna fires in Xingu, where changes in present-day risks exceed the changes in future risks (table 1). Nevertheless, future savanna fires' risk in Xingu are still projected to increase with higher warming levels.

In the Pantanal, fire risks increase most rapidly with global warming in forests, grassland and wetlands (figure 5 and table 1). In contrast, risk increases most rapidly with global warming for forest and farming fires in Xingu. The respective increase under a 1.5 °C, 2 °C and 3 °C warming is 10.3% (11.2%), 15.5% (16.5%) and 24.7% (25.3%) for forest fires (farming fires) in Xingu (figure 5(a) and table 1), and 13.6% (13.4%), 16.7% (16.6%) and 26.0% (24.8%) for forest fires (grassland and wetland fires) in the Pantanal (figure 5 and table 1), in comparison to the present-day risk (2001–2020).

Notwithstanding, constraining the global mean warming to +1.5 °C instead of +3.0 °C reduces the projected increase in fire risk by 14.4% (14.1%) for the Xingu forest fires (farming fires) and by 12.4% (11.4%) for forest fires (grassland and wetland fires) in the Pantanal (figures 5(c) and (f)). For savanna fires and farming fires in the Pantanal, the additional 1.5 °C of the +3 °C warming would lead

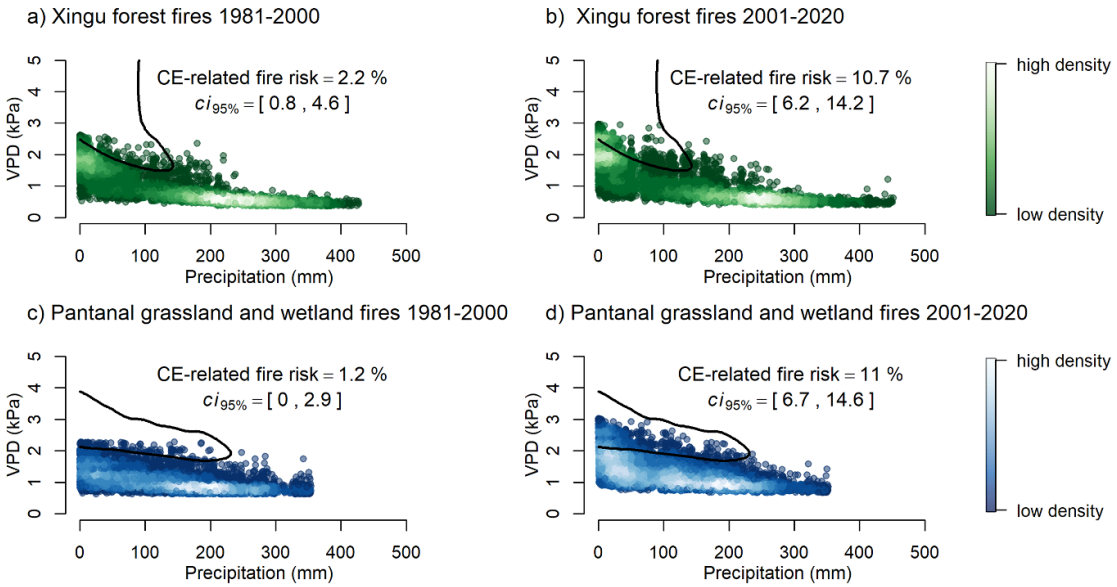

Figure 4. Likelihood of compound event-related (CE-related) fire risk. Empirical estimates of the CE-related fire risk during a past (left-side, 1981–2000) (a), (c) and a present period (right-side, 2001–2020) (b), (d) of forest fires in Xingu (top row, (a), (b)) and grassland and wetland fires in the Pantanal (bottom row, (c), (d)), based on 10 000 samples of VPD and precipitation (heatscatter points) drawn from their bivariate distribution describing the coupling between the hydrometeorological drivers. The black contour line indicates the critical threshold of impact, and the concurrent events of VPD and precipitation used to estimate CE-related fire risk are inside the critical impact contour line. The uncertainty associated with the parametric bivariate distribution is shown in terms of the 95% confidence interval ($ci_{95\%}$). The colour scale indicates increasing density of data points, based on a two-dimensional kernel estimator.

Table 1. Changes (%) in compound event-related (CE-related) fire risk from 1981–2000 to 2001–2020, and from 2001–2020 to the different warming levels of +1.5 °C, +2 °C and +3 °C. Third column indicates the difference between empirical estimates of CE-related fire risk from a past period (1981–2000) and present (2001–2020). Last three columns indicate the difference between the average empirical estimates of CE-related fire risk across the 14 ESMs (with MBC (multivariate bias-correction) of climate model's output) and the present risk obtained from 2001 to 2020. Uncertainty ranges are denoted in parenthesis in terms of the 95% confidence intervals (obtained as in figure 5).

Region	Fire type	2001–2020	+1.5 °C	+2 °C	+3 °C
Xingu	Forest	8.5 (3.8, 12.1)	10.3 (1.2, 22.9)	15.5 (4.2, 26.2)	24.7 (12.1, 31.7)
	Savanna	8.1 (4.2, 12.1)	5.7 (−3.3, 18.8)	6.0 (−4.2, 18.3)	7.0 (−4.2, 15.0)
	Farming	5.2 (1.7, 7.9)	11.2 (3.3, 22.5)	16.5 (5.4, 26.2)	25.3 (12.9, 31.7)
	Grassland and wetland	6.3 (1.7, 10.8)	3.6 (−6.7, 13.3)	2.3 (−7.5, 10.4)	−1.1 (−9.2, 7.9)
Pantanal	Forest	9.4 (5.0, 13.3)	13.6 (2.9, 30.0)	16.7 (3.3, 27.5)	26.0 (10.0, 41.7)
	Savanna	9.1 (5.0, 12.9)	11.5 (1.7, 27.1)	12.9 (2.1, 22.9)	18.5 (4.2, 34.6)
	Farming	9.3 (5.0, 13.3)	11.0 (1.2, 25.0)	13.5 (2.1, 23.3)	19.4 (5.0, 32.9)
	Grassland and wetland	9.8 (5.4, 13.8)	13.4 (2.1, 28.8)	16.6 (1.7, 27.5)	24.8 (9.6, 42.1)

to an increase of 7.0% and 8.4% of risk, respectively, thus highlighting the importance of not surpassing a global warming of 1.5 °C. In a similar way, the increase in risk for savanna fires in Xingu can be also reduced by 1.3% when constraining global mean warming to +1.5 °C instead of +3.0 °C (figure 5).

The best estimates of CE-related fire risks in figure 5 illustrate that the use of UBC methods can lead to a relative over- or underestimation of future climate-related fire risks (figure 5 grey and brown points). Uncertainties related to different bias-correction methods and the choices for the dependence structure are generally dominated by the increase in fire risk with global warming (figure 5). Despite the future changes in the dependence structure between VPD and precipitation under strong greenhouse gas forcing (tables S2 and S3), accounting for this bias in our projections did not alter our main conclusions (figure 5).

4. Discussion

Our results highlight the importance of constraining anthropogenic global warming to mitigate widespread fire impacts across two Brazilian biocultural heritage sites that are already ecologically and socially endangered. We provide evidence that the likelihood of major fires is already increasing and will keep increasing in the future. CE-related fire risks in Xingu (Pantanal) associated to forest (grassland and

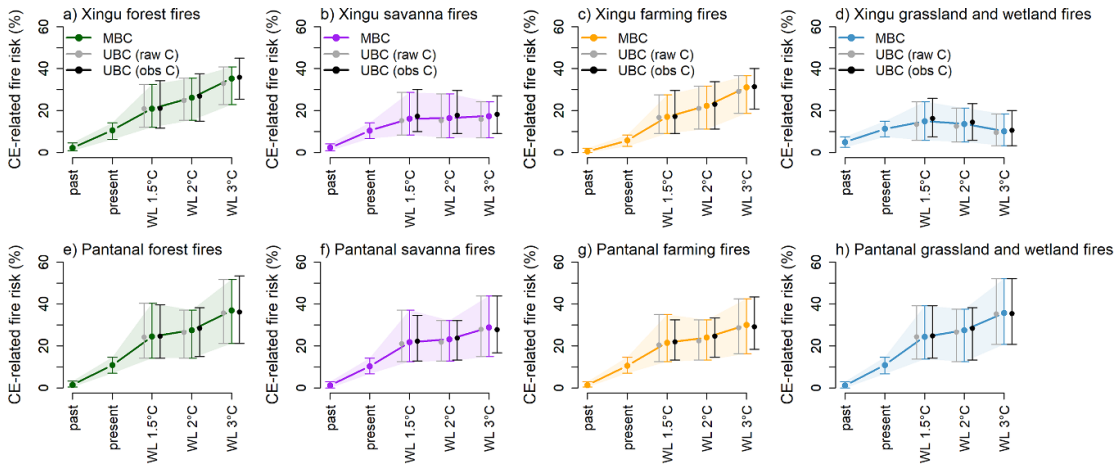

Figure 5. Projections of compound event-related (CE-related) fire risk under +1.5 °C, +2 °C and +3 °C warming levels. Empirical estimates of CE-related fire risk of forest fires (green dot line, (a), (e)), savanna fires (purple dot line, (b), (f)), farming fires (orange dot line, (c), (g)) and grassland and wetland fires (blue dot line, (d), (h)) in Xingu (top row, (a)–(d)) and the Pantanal (bottom row, (e)–(h)), using CMIP6 simulations of VPD and precipitation for different global mean warming levels. Grey and black values indicate the projections of CE-related fire risk obtained with UBC (univariate bias-correction) using the observed (obs C) and raw model (raw C) bivariate distribution, respectively, of VPD and precipitation. Coloured (i.e. not grey or black) full dotted lines indicate the empirical estimates of the CE-related fire risk with MBC (multivariate bias-correction) of the climate model's output. Shading illustrates the range of values among 14 ESMs, for both UBC and MBC methods. Uncertainty ranges illustrate the 95% confidence intervals associated with the copula modelling among the 14 ESMs.

wetland) fires have increased by 8.5% (9.8%) since 1981–2000 and might increase by 24.7% (24.8%) relative to present for +3 °C of global mean warming. However, constraining global warming to +1.5 °C instead of +3.0 °C potentially reduces the projected increase in CE-related fire risk by 11.4% in the Pantanal grassland and wetland fires, and by 14.4% in the Xingu forest fires. Also, in Xingu farming fires and Pantanal forest fires, potential reductions of 14.1% and 12.4% in the CE-related fire risk are projected if global warming is limited to +1.5 °C. To this purpose, the use of a compound event-oriented perspective [54–56] has proven valuable in this study, as the flammability of the Xingu and Pantanal regions is expected to increase due to the co-occurrence of drier and warmer climatic conditions caused by anthropogenic climate change.

Our study showed the exponential response of burned area to individual hydrometeorological variables, shaped by well-defined climate thresholds to fire occurrence. Even though the influence of VPD on burned area is found to be greater than all other predictor variables, the nonlinear relationship between burned area and climate is better explained by compound drivers representing air dryness and precipitation deficits (high VPD and low precipitation). It should be noted that high VPD may not only be a driver for plant stress, but can also be viewed as a diagnostic variable for these conditions as it increases when vegetation is water stressed and unable to sustain evapotranspiration [57, 58].

Drought and heat-related thresholds that trigger extremes of burned area are consistently lower in the Pantanal, than in Xingu (in both univariate and multivariate analyses). Further, the climate-change induced fire risks are also larger in the Pantanal than in Xingu. This is possibly related to the land covered with less fire-resistant forest vegetation in the Pantanal and, thus, the compound drought and heat stress does not require to be as extreme to trigger large fires. Nevertheless, if global warming is constrained to 1.5 °C, the projected CE-related fire risks may be reduced, an important ecological conservation action that could help to preserve the unique biodiversity of this biome.

In the Pantanal, the largest increase in CE-related fire risk with global mean warming primarily takes place across forest and grassland and wetlands, followed by savanna and farming fires. However, in Xingu, climate change is likely increasing fire risk more intensively in forest and farming areas, compared to savannas, grasslands and wetlands. Nevertheless, present-day climate change has already caused a significant increase in savanna fires (8.1%) in comparison to 1981–2000. With global mean warming, this CE-related fire risk in savannas will potentially remain constant.

The higher increase in CE-related fire risk in forest in comparison to savannas, is likely related to savannas high flammability compared with forests. Although forests are more resistant to fire due the humid fuel layer, an increase of forest fires in Xingu may accelerate the flammability of the landscape and possibly lead to a dieback of the tropical forests, causing a fourfold increase in tree mortality [10] and thus compromising the home and survival of the indigenous communities dependent on forest resources. The consequences could go beyond the limits of the

Xingu Indigenous Park, since the forests cool down the regional temperature by up to 5 °C [34].

The increasing farming fires in Xingu with global mean warming corroborate the consequences of the growing agricultural frontier in the Amazonia-Cerrado region. An indicator of the agricultural expansion in Xingu is the bimodal annual cycle of the farming fires in contrast to the other fire types, which may be attributed to the double cropping systems in expansion in this region (a soy-corn or soy-cotton rotation within one growing season). The second crop, usually corn, is very flammable at its last phenological stage. Also, in less technified farms, fire is still employed as land clearing tool.

In contrast to the other cases, grassland and wetland fires in Xingu are expected to decrease the burned area with global mean warming above +2 °C. This exception is most likely an artefact of the local likelihood Poisson regression in this case (both univariate and multivariate models). The lack of incorporating human influence into the statistical models might partially explain this lower performance. In addition, grassland and wetland fires were the least dominant fire type in this region, exhibiting an early peak of the fire season in comparison to the other fire types and are an exception to the leading exponential response of the burned area to individual hydrometeorological variables. Ideally, a more complex model incorporating human behaviour, ignition sources, legal and illegal deforestation, would better characterize fire regimes with more human influence, although the development of such models has been challenging and rare.

As an alternative to the conventional use of climate simulations as input of empirical or process-based models, we made use of parametric statistical modelling to assess CE-related fire risk. In addition, we have considered different ways to adjust climate model biases. We found that the use of univariate bias adjustment can lead to an over- or underestimation of future climate-related fire risks, despite the overall clear sign of climate-change induced risks, regardless of the bias-correction method employed. In fact, the way how climate models' biases affect the final risks is still a topic of discussion in the scientific community [59] and the way how changes in the dependence of the drivers will affect compound events in a warming world is a challenging task in assessing future climate risk of complex events.

The approach presented here is intended to address current challenges in describing the multivariate character of the climate thresholds beyond which the fire activity becomes extreme and on how climate change will affect fire risks induced by compound drought and atmospheric aridity. The focus on two main Brazilian biocultural heritage sites, constrains the challenges associated with interpretability and relevance of the study to the local scale. The action plan to preserve these biomes and the indigenous communities that depend on it must consider effective climate action to reduce greenhouse gas emissions as well as land-management policies towards the combat of illegal deforestation and logging, to reduce ignition sources and to slow-down feedbacks that lead to the degradation/disturbance of the ecosystems.

5. Conclusions

Our results indicate that concurrent extreme VPD and precipitation conditions are key drivers for fire occurrence in both regions. The impact of atmospheric dryness is greater than deficits in precipitation, and more relevant in the Pantanal than in Xingu. The effects of global warming in terms of CE-related fire risk are projected to be experienced in both regions, but to a larger extent in the Pantanal. Nevertheless, constraining global warming to +1.5 °C instead of +3.0 °C reduces the projected increase in fire risk by 12.4% (11.4%) in the case of forest fires (grassland and wetland fires) in the Pantanal, and by 14.4% (14.1%) in the case of forest fires (farming fires) in Xingu. Effective climate action to reduce greenhouse gas emissions and slow down the rate of warming should therefore act in concert with sound fire management and environmental protection of the biodiversity and indigenous communities that safeguard the forests and hold unique knowledge about sustainable practices. If we do not achieve the 'full potential' for climate change and follow more effective ways in preventing and controlling fires and sustainable uses of land, we might prevent tipping events consequences that threaten these sites and the world. This demands being able to predict where and when major fires may occur in the time frame that allows managers to act in a proactive way and create synergies between scientific, local, and indigenous knowledge.

Data availability statement

The data that support the findings of this study are openly available at the following URL/DOI: the MODIS-derived MCD64A1 monthly burned area product 10.5067/MODIS/MCD64A1.006 [39] and the annual MapBiomas land-cover maps [40] (https://mapbiomas.org) are openly available and were here assessed through the Google Earth Engine (GEE). The ERA5-Land [41] is openly available by the Copernicus Climate Data Store (https://cds.climate.copernicus.eu/cdsapp#!/dataset/reanalysis-era5-land), the GRACE-based reconstructed TWS is openly available by [42] (https://figshare.com/articles/dataset/GRACE-REC_A_reconstruction_of_climate-driven_water_storage_changes_over_the_last_century/7670849) and the CMIP6 next generation (CMIP6ng) archive is provided

by [46] (https://zenodo.org/record/3734128#.YYuvOmDMJaQ).

Acknowledgments

The authors acknowledge the COST Action DAMOCLES (CA17109). This work was supported by the Swiss National Science Foundation (SNSF) Project Nos. 186282 and 179876. Jakob Zscheischler acknowledges the Helmholtz Initiative and Networking Fund (Young Investigator Group COMPOUNDX; Grant Agreement No. VH-NG-1537). Paulo M Brando acknowledges the National Science Foundation #s 2001184 & 1802754 and the Conselho Nacional de Desenvolvimento Científico e Tecnológico—CNPq/Prevfogo-Ibama (#442710/2018-6). We acknowledge the World Climate Research Programme (WCRP)'s Working Group on Coupled Modelling responsible for the CMIP6. Andreia F S Ribeiro is sincerely thankful to Sofia Ermida for the helpful insights on Google Earth Engine (GEE).

Authors' contribution

Andreia F S Ribeiro, Paulo M Brando, Ludmila Rattis, Sonia I Seneviratne and Jakob Zscheischler conceived the idea, Andreia F S Ribeiro conducted the analysis and wrote the first draft of the manuscript, Lucas Santos, Mathias Hauser and Martin Hirschi instructed the acquisition and processing of the data, Paulo M Brando and Jakob Zscheischler supervised the overall work. All authors reviewed and finalized the manuscript.

ORCID iDs

Andreia F S Ribeiro https://orcid.org/0000-0003-0481-0337
Paulo M Brando https://orcid.org/0000-0001-8952-7025
Lucas Santos https://orcid.org/0000-0003-0615-2315
Ludmila Rattis https://orcid.org/0000-0001-6943-3099
Martin Hirschi https://orcid.org/0000-0001-9154-756X
Mathias Hauser https://orcid.org/0000-0002-0057-4878
Sonia I Seneviratne https://orcid.org/0000-0001-9528-2917
Jakob Zscheischler https://orcid.org/0000-0001-6045-1629

References

[1] Berenguer E, Carvalho N, Anderson L O, Aragão L E O C, França F and Barlow J 2021 Improving the spatial-temporal analysis of Amazonian fires *Glob. Change Biol.* **27** 469–71
[2] Simoes R, Picoli M C A, Camara G, Maciel A, Santos L, Andrade P R, Sánchez A, Ferreira K and Carvalho A 2020 Land use and cover maps for Mato Grosso State in Brazil from 2001 to 2017 *Sci. Data* **7** 1–10
[3] Panday P K *et al* 2015 Deforestation offsets water balance changes due to climate variability in the Xingu River in eastern Amazonia *J. Hydrol.* **523** 822–9
[4] Soares-Filho B *et al* 2012 Forest fragmentation, climate change and understory fire regimes on the Amazonian landscapes of the Xingu headwaters *Landsc. Ecol.* **27** 585–98
[5] Marengo J A *et al* 2021 Extreme drought in the Brazilian Pantanal in 2019–2020: characterization, causes, and impacts *Front. Water* **3** 639204
[6] Lewis S L, Brando P M, Phillips O L, van der Heijden G M F and Nepstad D 2011 The 2010 Amazon drought *Science* **331** 554
[7] Kruid S, Macedo M N, Gorelik S R, Walker W, Moutinho P, Brando P M, Castanho A, Alencar A, Baccini A and Coe M T 2021 Beyond deforestation: carbon emissions from land grabbing and forest degradation in the Brazilian Amazon *Front. For. Glob. Change* **4** 645282
[8] Brando P M, Soares-Filho B, Rodrigues L, Assunção A, Morton D, Tuchschneider D, Fernandes E C M, Macedo M N, Oliveira U and Coe M T 2020 The gathering firestorm in southern Amazonia *Sci. Adv.* **6** 1–10
[9] Berenguer E *et al* 2021 Tracking the impacts of El Niño drought and fire in human-modified Amazonian forests *Proc. Natl Acad. Sci.* **118** e2019377118
[10] Brando P M *et al* 2014 Abrupt increases in Amazonian tree mortality due to drought-fire interactions *Proc. Natl Acad. Sci. USA* **111** 6347–52
[11] Aragão L E O C, Malhi Y, Roman-Cuesta R M, Saatchi S, Anderson L O and Shimabukuro Y E 2007 Spatial patterns and fire response of recent Amazonian droughts *Geophys. Res. Lett.* **34** 1–5
[12] Brando P, Macedo M, Silvério D, Rattis L, Paolucci L, Alencar A, Coe M and Amorim C 2020 Amazon wildfires: scenes from a foreseeable disaster *Flora Morphol. Distrib. Funct. Ecol. Plants* **268** 151609
[13] Moura L C, Scariot A O, Schmidt I B, Beatty R and Russell-Smith J 2019 The legacy of colonial fire management policies on traditional livelihoods and ecological sustainability in savannas: impacts, consequences, new directions *J. Environ. Manage.* **232** 600–6
[14] Silvério D V, Oliveira R S, Flores B M, Brando P M, Almada H K, Furtado M T, Moreira F G, Heckenberger M, Ono K Y and Macedo M N Anon 2022 Intensification of fire regimes and forest loss in the Território Indígena do Xingu *Environ. Res. Lett.* **17** 045012
[15] Garcia L C *et al* 2021 Record-breaking wildfires in the world's largest continuous tropical wetland: integrative fire management is urgently needed for both biodiversity and humans *J. Environ. Manage.* **293** 112870
[16] Libonati R, Dacamara C C, Peres L F, de Carvalho L A S and Garcia L C 2020 Rescue Brazil's burning Pantanal wetlands *Nature* **588** 217–9
[17] Pletsch M A J S, Silva Junior C H L, Penha T V, Körting T S, Silva M E S, Pereira G, Anderson L O and Aragão L E O C 2021 The 2020 Brazilian pantanal fires *An. Acad. Bras. Cienc.* **93** 2020–2
[18] Miranda C D S, Paranho Filho A C and Pott A 2018 Mudanças na cobertura da vegetação do pantanal dectadas por índice de vegetação: uma estratégia de conservação *Biota Neotrop* **18** 1–6
[19] Tomas W M *et al* 2021 Distance sampling surveys reveal 17 million vertebrates directly killed by the 2020's wildfires in the Pantanal *Braz. Sci. Rep.* **11** 1–8
[20] Zhou S, Zhang Y, Williams A P and Gentine P 2019 Projected increases in intensity, frequency, and terrestrial carbon costs of compound drought and aridity events *Sci. Adv.* **5** 1–9

[21] Seneviratne S I et al Weather and climate extreme events in a changing climate IPCC, 2021: Summary for Policymakers. In: Climate Change 2021: The Physical Science Basis. Contribution of Working Group I to the Sixth Assessment Report of the Intergovernmental Panel on Climate Change ed V Masson-Delmotte et al 2021 (Cambridge: Cambridge University Press) ch 11 (available at: www.ipcc.ch/report/ar6/wg1/downloads/report/IPCC_AR6_WGI_Chapter_11.pdf) accepted
[22] Butt E W, Conibear L, Knote C and Spracklen D V 2021 Large air quality and public health impacts due to Amazonian deforestation fires in 2019 GeoHealth 5 e2021GH000429
[23] Lima C H R, AghaKouchak A and Randerson J T 2018 Unraveling the role of temperature and rainfall on active fires in the Brazilian Amazon using a nonlinear Poisson model J. Geophys. Res. Biogeosci. 123 117–28
[24] Fernandes K, Verchot L, Baethgen W, Gutierrez-Velez V, Pinedo-Vasquez M and Martius C 2017 Heightened fire probability in Indonesia in non-drought conditions: the effect of increasing temperatures Environ. Res. Lett. 12 054002
[25] Sutanto S J, Vitolo C, di Napoli C, D'Andrea M and van Lanen H A J 2020 Heatwaves, droughts, and fires: exploring compound and cascading dry hazards at the pan-European scale Environ. Int. 134 105276
[26] Turco M, Jerez S, Augusto S, Tarín-Carrasco P, Ratola N, Jiménez-Guerrero P and Trigo R M 2019 Climate drivers of the 2017 devastating fires in Portugal Sci. Rep. 9 1–8
[27] Gouveia C M, Bistinas I, Liberato M L R, Bastos A, Koutsias N and Trigo R 2016 The outstanding synergy between drought, heatwaves and fuel on the 2007 Southern Greece exceptional fire season Agric. For. Meteorol. 218–219 135–45
[28] Miralles D G, Gentine P, Seneviratne S I and Teuling A J 2019 Land–atmospheric feedbacks during droughts and heatwaves: state of the science and current challenges Ann. New York Acad. Sci. 1436 19–35
[29] Zscheischler J and Seneviratne S I 2017 Dependence of drivers affects risks associated with compound events Sci. Adv. 3 1–11
[30] Salvadori G, Durante F, de Michele C, Bernardi M and Petrella L 2016 A multivariate copula-based framework for dealing with hazard scenarios and failure probabilities J. Am. Water Resour. Assoc. 5 2
[31] Brando P M, Goetz S J, Baccini A, Nepstad D C, Beck P S A and Christman M C 2010 Seasonal and interannual variability of climate and vegetation indices across the Amazon Proc. Natl Acad. Sci. USA 107 14685–90
[32] Silva P S, Bastos A, Libonati R, Rodrigues J A and DaCamara C C 2019 Impacts of the 1.5 °C global warming target on future burned area in the Brazilian Cerrado For. Ecol. Manage. 446 193–203
[33] Castanho A D A, Coe M T, Brando P, Macedo M, Baccini A, Walker W and Andrade E M 2020 Potential shifts in the aboveground biomass and physiognomy of a seasonally dry tropical forest in a changing climate Environ. Res. Lett. 15 34053
[34] Silvério D V, Brando P M, Macedo M N, Beck P S A, Bustamante M and Coe M T 2015 Agricultural expansion dominates climate changes in southeastern Amazonia: the overlooked non-GHG forcing Environ. Res. Lett. 10 104015
[35] Rattis L, Brando P, Macedo M, Spera S, Castanho A, Marques E, Queiroz N, Silvério D and Coe M 2021 Climatic limit for agriculture in Brazil Nat. Clim. Change 11 1098–104
[36] Dias L C P, Macedo M N, Costa M H, Coe M T and Neill C 2015 Effects of land cover change on evapotranspiration and streamflow of small catchments in the Upper Xingu River Basin, Central Brazil J. Hydrol. Reg. Stud. 4 108–22
[37] MapBiomas Fogo 2021 Mapbiomas Fogo—As Cicatrizes Deixadas Pelo Fogo No Mapbiomas pp 1–10 (available at: https://mapbiomas-br-site.s3.amazonaws.com/Fact_Sheet.pdf)
[38] Berlinck C N, Lima L H A, Pereira A M M, Carvalho E A R, Paula R C, Thomas W M and Morato R G 2020 The pantanal is on fire and only a sustainable agenda can save the largest wetland in the world Braz. J. Biol. 82 2–3
[39] Giglio L, Boschetti L, Roy D P, Humber M L and Justice C O 2018 The Collection 6 MODIS burned area mapping algorithm and product Remote Sens. Environ. 217 72–85
[40] Mapbiomas Collection 6 of the Annual Series of Land Use and Land Cover Maps of Brazil 2021 (available at: www.mapbiomas.org)
[41] Muñoz-Sabater J et al 2021 ERA5-Land: a state-of-the-art global reanalysis dataset for land applications Earth Syst. Sci. Data 13 4349–83
[42] Humphrey V and Gudmundsson L 2019 GRACE-REC: a reconstruction of climate-driven water storage changes over the last century Earth Syst. Sci. Data 11 1153–70
[43] Eyring V, Bony S, Meehl G A, Senior C A, Stevens B, Stouffer R J and Taylor K E 2016 Overview of the Coupled Model Intercomparison Project Phase 6 (CMIP6) experimental design and organization Geosci. Model Dev. 9 1937–58
[44] O'Neill B C et al 2016 The scenario model intercomparison project (ScenarioMIP) for CMIP6 Geosci. Model Dev. 9 3461–82
[45] Hauser M, Engelbrecht F and Fischer E 2021 Transient global warming levels for CMIP5 and CMIP6 (v0.2.0) Zenodo [Data set]
[46] Brunner L, Hauser M, Lorenz R and Beyerle U 2020 The ETH Zurich CMIP6 next generation archive: technical documentation p 10
[47] Wartenburger R, Hirschi M, Donat M G, Greve P, Pitman A J and Seneviratne S I 2017 Changes in regional climate extremes as a function of global mean temperature: an interactive plotting framework Geosci. Model Dev. 10 3609–34
[48] Loader C, Sun J, Technologies L and Liaw A 2020 Package 'locfit' (available at: https://cran.r-project.org/web/packages/locfit/)
[49] Loader C 1999 Local regression and likelihood J. Am. Stat. Assoc. 96 339–55
[50] Brando P M, Oliveria-Santos C, Rocha W, Cury R and Coe M T 2016 Effects of experimental fuel additions on fire intensity and severity: unexpected carbon resilience of a neotropical forest Glob. Change Biol. 22 2516–25
[51] Ribeiro A F S, Russo A, Gouveia C M, Páscoa P and Zscheischler J 2020 Risk of crop failure due to compound dry and hot extremes estimated with nested copulas Biogeosciences 17 4815–30
[52] Cannon A J, Sobie S R and Murdock T Q 2015 Bias correction of GCM precipitation by quantile mapping: how well do methods preserve changes in quantiles and extremes? J. Clim. 28 6938–59
[53] Cannon A J 2018 Multivariate quantile mapping bias correction: an N-dimensional probability density function transform for climate model simulations of multiple variables Clim. Dyn. 50 31–49
[54] Bevacqua E et al 2021 Guidelines for studying diverse types of compound weather and climate events Earths Future 9 1–23
[55] Zscheischler J et al 2020 A typology of compound weather and climate events Nat. Rev. Earth Environ. 1 333–47

[56] Zscheischler J et al 2018 Future climate risk from compound events Nat. Clim. Change 8 469–77
[57] Seneviratne S I, Corti T, Davin E L, Hirschi M, Jaeger E B, Lehner I, Orlowsky B and Teuling A J 2010 Investigating soil moisture-climate interactions in a changing climate: a review Earth Sci. Rev. 99 125–61
[58] Liu L, Gudmundsson L, Hauser M, Qin D, Li S and Seneviratne S I 2020 Soil moisture dominates dryness stress on ecosystem production globally Nat. Commun. 11 1–9
[59] Villalobos-Herrera R, Bevacqua E, Ribeiro A F S, Auld G, Crocetti L, Mircheva B, Ha M, Zscheischler J and de Michele C 2021 Towards a compound-event-oriented climate model evaluation: a decomposition of the underlying biases in multivariate fire and heat stress hazards Nat. Hazards Earth Syst. Sci. 21 1867–85